

A significant influence of the substrate on the magnetic anisotropy of monatomic nanowires

Matej Komelj,^{1,*} Daniel Steiauf,² and Manfred Fähnle²

¹*Jožef Stefan Institute, Jamova 39, SI-1000 Ljubljana, Slovenia*

²*Max-Planck-Institut für Metallforschung, Heisenbergstraße 3, D-70569 Stuttgart, Germany*

(Dated: December 25, 2021)

The magnetic anisotropy energy of Fe and Co monatomic nanowires both free-standing and at the step edge of a Pt surface is investigated within the framework of the density-functional theory and local-spin-density (LSDA) approximation. Various types of the analysis of the calculated data reveal that the spin-orbit interaction of the Pt atoms and the hybridization between the electronic states have an important impact on the direction of the easy axis and on the magnitude of the magnetic anisotropy, both by a direct contribution localized at the Pt atoms and by an indirect contribution due to the modification of the Co-localized part via hybridization effects.

PACS numbers: 75.75.+a, 75.30.Gw, 71.15.Mb

I. INTRODUCTION

The experimentally observed existence of ferromagnetism in linear chains of Co atoms, grown at a step edge of a Pt(997) surface terrace¹, motivated several theoretical investigations which were aimed to interpret the measured large orbital contribution to the magnetic moments^{2,3}, and the magnetic anisotropy^{4,5,6,7,8,9}. The latter is distinguished by the experimentally found easy axis along the direction perpendicular to the Co wire, shifted by 43° from the surface normal towards the Pt step edge, and by the magnetic-anisotropy energy (MAE) of the order of 2 meV/Co atom. This value is a factor of about 50 larger than the one of hcp Co (which is already large for a transitional metal). Various theoretical attempts to reproduce the experimental findings yielded quantitatively different results. Hong and Wu⁴ performed the full-potential linearized-augmented-plane-waves (FLAPW) calculation for infinite Co wires on the flat Pt(001) and Cu(001) substrates. They found that the MAE magnitude was enhanced when they replaced the Cu substrate by platinum due to the strong spin-orbit coupling (SOC) of Pt atoms. They obtained the easy axis along the wire in the case of the Cu(001) substrate, and perpendicular to the wire in the plane of the Pt(001) substrate. They also noticed a certain sensitivity of the results on the size of the supercell. The results of the Korringa-Kohn-Rostoker (KKR) calculations^{5,6} on finite (up to 10 atoms) Co wires along a step edge of a Pt(111) surface were in remarkable agreement with the experiment. However, to some extent, this agreement might be coincidental since the atomic-sphere approximation (ASA) was applied for the potential. Again, the authors ascribed the peculiar magnetic anisotropy to the influence of the Pt substrate. The same conclusion was drawn also on the basis of the FLAPW calculations for the infinite Co^{7,8,9} and Fe⁸ wires at the Pt(111) step edge by analyzing the data in the frame of a symmetry-based “atomic-pair” model. Although shape approximations were not applied for the potential, the experimental easy

axis was not reproduced as good as in the case of the KKR ASA calculation^{5,6}, even if the structural relaxations were taken into account⁹. Finally, an FLAPW calculation¹⁰ for a considerably larger supercell as used in Ref. 9, including structural relaxations, found an easy axis which is in a plane parallel to the substrate surface and almost perpendicular to the wire, in contrast to the result of Ref. 9 and to the experimental result. All this indicates that the orientation of the calculated easy axis depends extremely sensitively on the calculational details. We therefore do not take the enormous effort to converge the results with respect to all parameters of the calculation (e.g., geometry and size of the supercell), but we concentrate on the physical interpretation of the results concerning the influence of the Pt substrate by means of two different types of the analysis.

II. CALCULATIONAL METHOD

We performed the calculations with the FLAPW¹¹ Wien97¹² code by using the local-spin-density approximation (LSDA)¹³ for the exchange-correlation potential. The SOC contribution was added to the Hamiltonian in terms of the second-variational method^{14,15}. In the implementation of Ref. 12 SOC is taken into account just within muffin-tin spheres but not in the interstitial region. The energy difference in the total energy due to different magnetization directions was determined according to the magnetic force theorem^{16,17}. In this approximation, first a self-consistent effective potential $V_{\text{eff}}^{(0)}$ is determined for an initial magnetic configuration (0) of the system. In a subsequent step the eigenvalues are determined for respectively two different orientations (1) and (2) of the magnetization by respectively one single diagonalization of the Hamiltonian for the same fixed potential $V_{\text{eff}}^{(0)}$ but with the SOC term corresponding to the two orientations of the magnetization. The magnetic anisotropy energy e_{MCA} which is defined as the difference in the total energy for the two magnetization directions

FIG. 1: Comparison between total energy differences e_{MCA} and force theorem results $e_{\text{MCA}}^{\text{ft}}$ from LMTO-ASA calculations. The total energy (symbol \circ) was obtained with $20 \times 4 \times 1$ (dashed line) and $32 \times 6 \times 1$ (solid line) k points for the sampling of the Brillouin zone. All the force-theorem calculations were done with $32 \times 6 \times 1$ k points, starting from a potential $V_{\text{eff}}^{(0)}$ created with $20 \times 4 \times 1$ k points. The \diamond starting potential was without SOC, while the $+$ starting potentials included SOC with the magnetization in different directions ($\phi = 0^\circ, \pm 90^\circ, 180^\circ$ with $\theta = 0^\circ$; and $\theta = 90^\circ$ with $\phi = 0^\circ$).

is then approximated by the difference in the respective sums of eigenvalues:

$$e_{\text{MCA}}^{\text{ft}} = \int_{-\infty}^{E_F^{(2)}} \epsilon \mathcal{N}^{(2)}(\epsilon) d\epsilon - \int_{-\infty}^{E_F^{(1)}} \epsilon \mathcal{N}^{(1)}(\epsilon) d\epsilon, \quad (1)$$

In eq. (1) the functions $\mathcal{N}^{(1)}(\epsilon)$ and $\mathcal{N}^{(2)}(\epsilon)$ are the electronic density of states for the two orientations, and $E_F^{(1)}$ and $E_F^{(2)}$ are the respective Fermi levels, which are calculated from the number Z of the valence electrons according to:

$$Z = \int_{-\infty}^{E_F^{(i)}} \mathcal{N}^{(i)}(\epsilon) d\epsilon. \quad (2)$$

The convergence of the magnetic anisotropy energy with respect to the number of k points used for the sampling of the Brillouin zone is notoriously bad. However, it turns out that less k points are needed for the calculation of $V_{\text{eff}}^{(0)}$. Hence, the advantage of the magnetic force theorem is that the calculation of $e_{\text{MCA}}^{\text{ft}}$ from (1) requires considerably less computational power than the determination of the respective difference in the total energy, obtained from two self-consistent calculations. Because the FLAPW method is very time consuming, the application of the force theorem is desirable. An open question thereby is how to select the initial configuration (0) for the determination of $V_{\text{eff}}^{(0)}$ in order to minimize the difference between e_{MCA} and $e_{\text{MCA}}^{\text{ft}}$. To figure this out we have calculated by means of the linear-muffin-tin-orbital (LMTO) method in atomic-sphere approximation¹⁸ both e_{MCA} (which is possible because LMTO-ASA is much faster, albeit less accurate, than FLAPW) and $e_{\text{MCA}}^{\text{ft}}$ for various configurations (0). It turns out that it is absolutely indispensable to include SOC for the initial configuration. The initial orientation of the magnetization has only a subtle effect on $e_{\text{MCA}}^{\text{ft}}$ since for each orientation the agreement between e_{MCA} and $e_{\text{MCA}}^{\text{ft}}$ is nearly perfect as presented in Fig. 1. For this test, the infinite Co nanowire at the step edge of the Pt(111) surface was modelled by a supercell with the geometry from Ref. 7, which contains 16 atoms (15 Pt + one Co atom) and 8 empty atomic spheres that are required due to the ASA approximation.

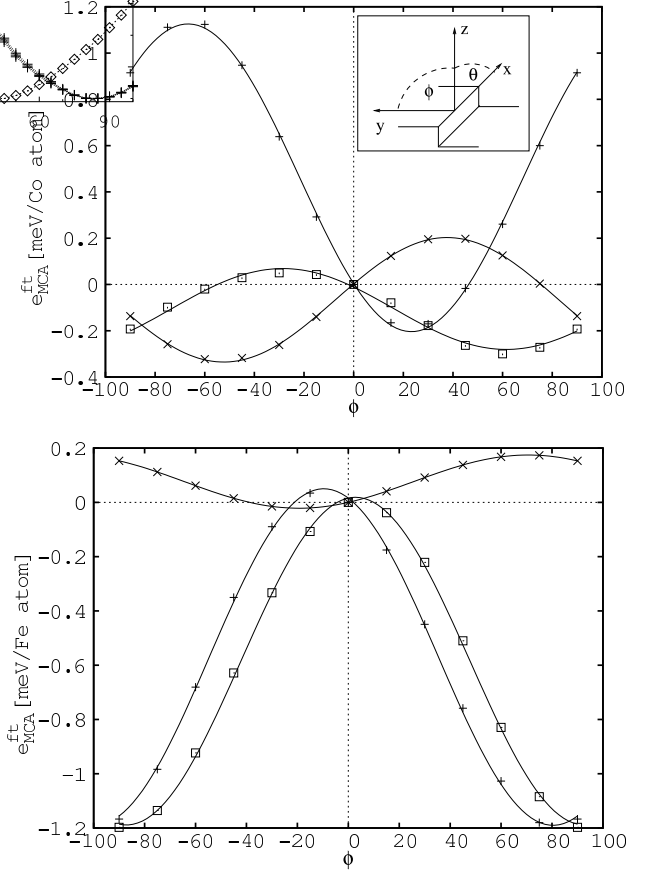


FIG. 2: The calculated energy difference $e_{\text{MCA}}^{\text{ft}} = e(\theta = 0^\circ, \phi) - e(\theta = 0^\circ, \phi = 0^\circ)$ for the Co (top) and the Fe (bottom) Pt-supported wire with SOC at all sites $+$ or just at the Co(Fe) \times or Pt \square atoms.

The rest of the calculations were performed for a monatomic wire at the step edge of a Pt surface described by a supercell of 13 atoms (12 Pt + one Co or Fe atom) by adopting the experimental lattice parameters of fcc Pt (for details, see Ref. 2). In addition, freestanding wires were considered by removing all Pt atoms from the supercell. The orientation of the coordinate system was adopted from Refs. 7, 8, 9 (see the inset in Fig. 2). The cut-off parameter for the plane-wave expansion was set to 7.3 Ry. The Brillouin-zone (BZ) integration was carried out by both the modified tetrahedron¹⁹ and the Gaussian smearing²⁰ methods with 45 (40 in the case of the freestanding wires) k -points in the full BZ for the self-consistent part and 192 (184) for the force-theorem part of the calculation as determined on the basis of convergence tests.

We calculated $e_{\text{MCA}}^{\text{ft}}$ for the magnetization confined either to the yz (the angle ϕ , Fig. 2) or the xz plane (the angle θ , Fig. 3) with respect to the energy for the case of the magnetization along the z axis. The calculated data were fitted by the functions $a - b \cos^2(\phi - c)$ and $a - b \cos^2(\theta)$ for the respective planes. Since there is a quantitative deviation from the results obtained by Shick *et al.*^{7,8} for a slightly different supercell, we performed a

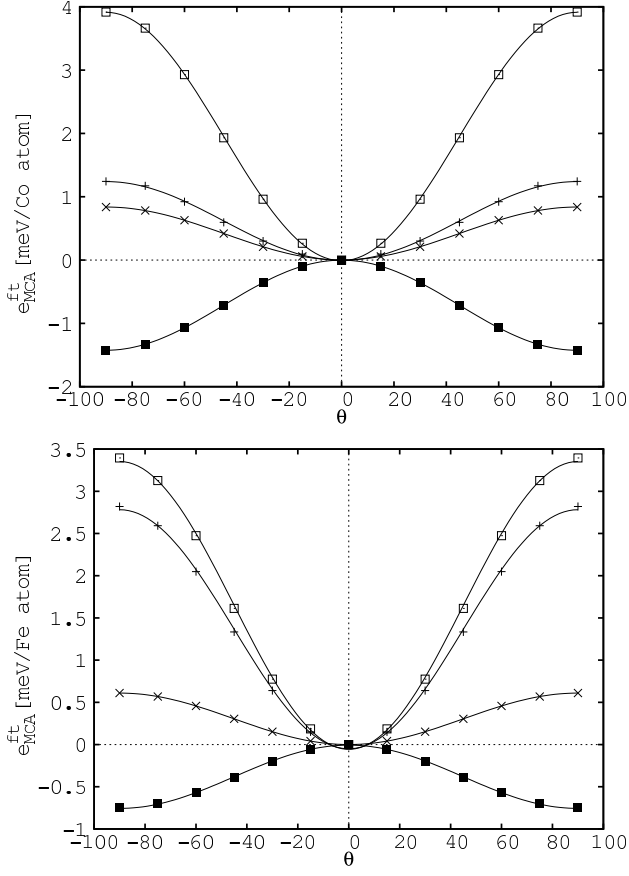


FIG. 3: The calculated energy difference $e_{\text{MCA}}^{\text{ft}} = e(\theta, \phi = 0^\circ) - e(\theta = 0^\circ, \phi = 0^\circ)$ for the Co (top) and the Fe (bottom) Pt-supported wire with SOC at all sites + or just at the Co(Fe) \times or Pt \square atoms. The symbols \blacksquare present the respective energy difference for the freestanding wires.

test calculation with their type of the supercell (16 atoms but considerably less vacuum at the top of the (111) surface), and we could satisfactorily reproduce the published results from Refs. 7,8. This demonstrates that different computer codes give the same results, and it confirms the findings from previous investigations that the magnetic anisotropy depends extremely sensitively on the details of the structural model.

To explore the influence of the Pt substrate we performed two types of the analysis:

(a) The densities of states $\mathcal{N}^{(1,2)}(\epsilon)$ in eq. (1) can be subdivided into the contributions $\mathcal{N}_j^{(1,2)}(\epsilon)$ which correspond to the respective projections onto the Co (Fe) atoms ($j = 1$) and Pt atoms ($j = 2$) muffin-tin spheres. This subdivision yields $e_{\text{MCA}}^{\text{ft,Co}}$ ($e_{\text{MCA}}^{\text{ft,Fe}}$) and $e_{\text{MCA}}^{\text{ft,Pt}}$. Because the total $e_{\text{MCA}}^{\text{ft}}$ contains also the contribution from the interstitial region between the muffin-tin spheres, we cannot expect that the sum $e_{\text{MCA}}^{\text{ft,Co}} + e_{\text{MCA}}^{\text{ft,Pt}}$ is equal to $e_{\text{MCA}}^{\text{ft}}$. In the following we call $e_{\text{MCA}}^{\text{ft,Pt}}$ the “direct contribution” of the Pt atoms to the magnetic anisotropy energy, because it is directly assigned to the Pt sites. Within the framework of the rigid band model we can

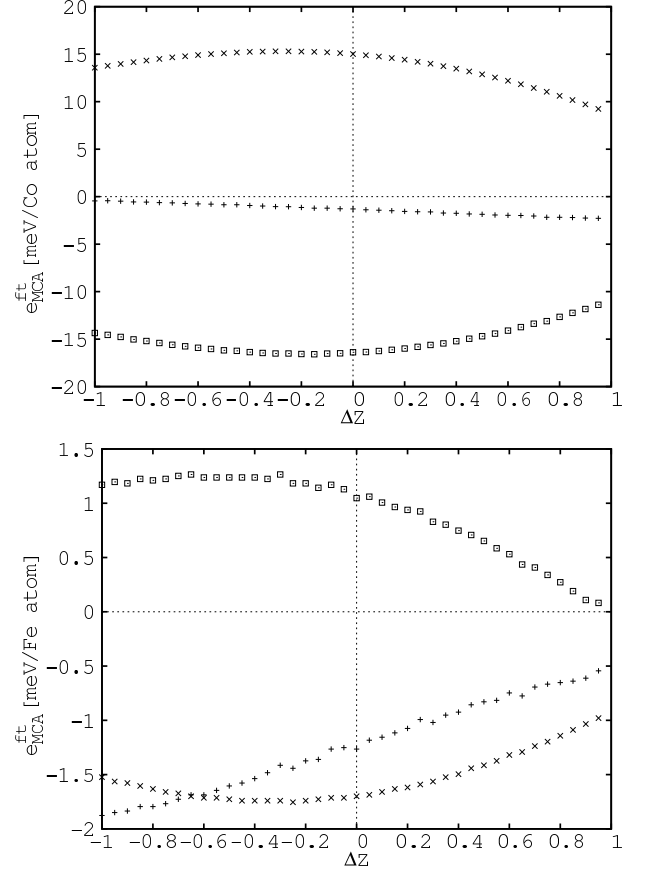


FIG. 4: The calculated magnetic anisotropy energy $e_{\text{MAE}}^{\text{ft}} = e(\theta = 0^\circ, \phi = 22.85^\circ) - e(\theta = 0^\circ, \phi = -67.15^\circ)$ for the Co wire (top) and $e_{\text{MAE}}^{\text{ft}} = e(\theta = 0^\circ, \phi = 80.40^\circ) - e(\theta = 0^\circ, \phi = -9.60^\circ)$ for the Fe wire (bottom); total contribution (+), Co (Fe) contribution (\times), Pt contribution (\square).

determine these quantities as a function of the band filling $Z + \Delta Z$, where Z denotes the band filling for the real system. The change in the band filling leads to the shifts in the Fermi levels appearing in eq. (1) as: $Z + \Delta Z = \int_{-\infty}^{E_F^{(1,2)} + \Delta E_F^{(2,1)}} \mathcal{N}^{(1,2)}(\epsilon) d\epsilon$. The results of this analysis are presented in Figs. 4,5.

(b) In addition to the calculation with SOC for all atoms, we performed calculations where we switched off the SOC term for the Co(Fe) atoms or for the Pt atoms, respectively. Thereby we changed the hybridization between the electronic states at various sites and hence the eigenvalues for the two orientations. Switching off the SOC term at say the Pt atoms does not mean that there is no longer the $e_{\text{MCA}}^{\text{ft,Pt}}$ contribution because there is still a difference in the Pt-projected density of states for the two magnetization directions due to the hybridization of the Pt-localized orbitals with the Co-localized orbitals. And, vice versa, when switching on the very large SOC term at the Pt atoms the hybridization of the Co-localized orbitals with the Pt-localized orbitals changes drastically and this has a large effect on $e_{\text{MCA}}^{\text{ft,Co}}$. In the following we call this the “indirect contribution” of the Pt atoms

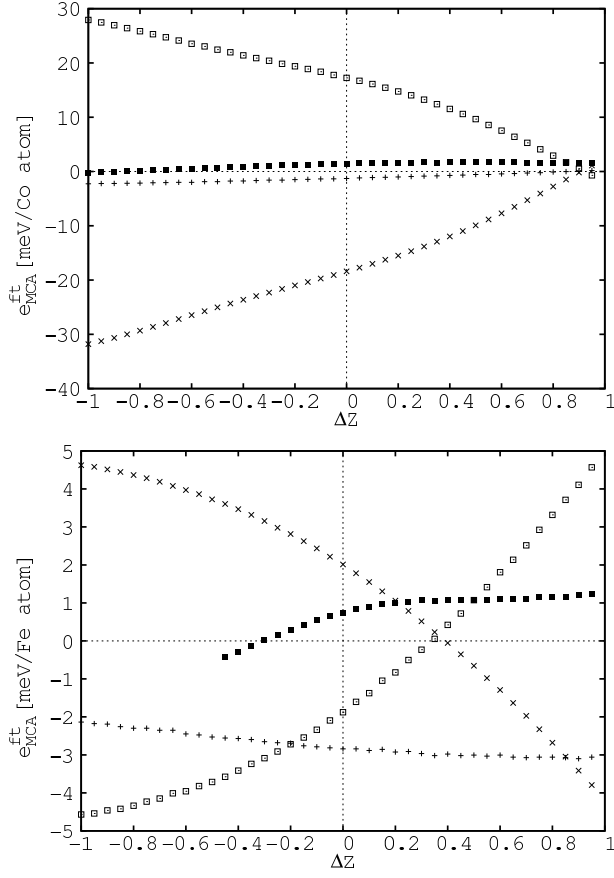


FIG. 5: The calculated magnetic anisotropy energy $e_{\text{MAE}} = e(\theta = 0^\circ, \phi = 0^\circ) - e(\theta = 90^\circ, \phi = 0^\circ)$ for the Co (top) and the Fe (bottom) wire; total contribution (+), Co (Fe) contribution (x), Pt contribution □, free-standing wire (■).

to the magnetic anisotropy energy. The results of such analysis are presented in Figs. 6,7.

III. DISCUSSION

By looking at Fig. 3 it becomes immediately clear that there is a big influence of the Pt substrate. Whereas for the free-standing wire the easy axis is in the wire direction, it is perpendicular to the wire direction for the Pt-supported systems. Furthermore, there is a big difference between the Pt-supported Co and Fe wires concerning the orientation of the easy axis in the plane perpendicular to the wire, see Fig. 2. Whereas for the Fe wire the easy axis is nearly perpendicular to the surface normal, it is inclined by an angle of 22.85° from the surface normal towards the step edge in the case of the Co wire. Remember that for the chains of Co atoms at the step edge of Pt(997) an angle of 43° was found experimentally¹. The difference in the energy between the easy and the hard axis in the plane perpendicular to the wire is about 1.3 meV per Co or per Fe atom, whereas the experimental value is about 2 meV per Co atom¹. In the following

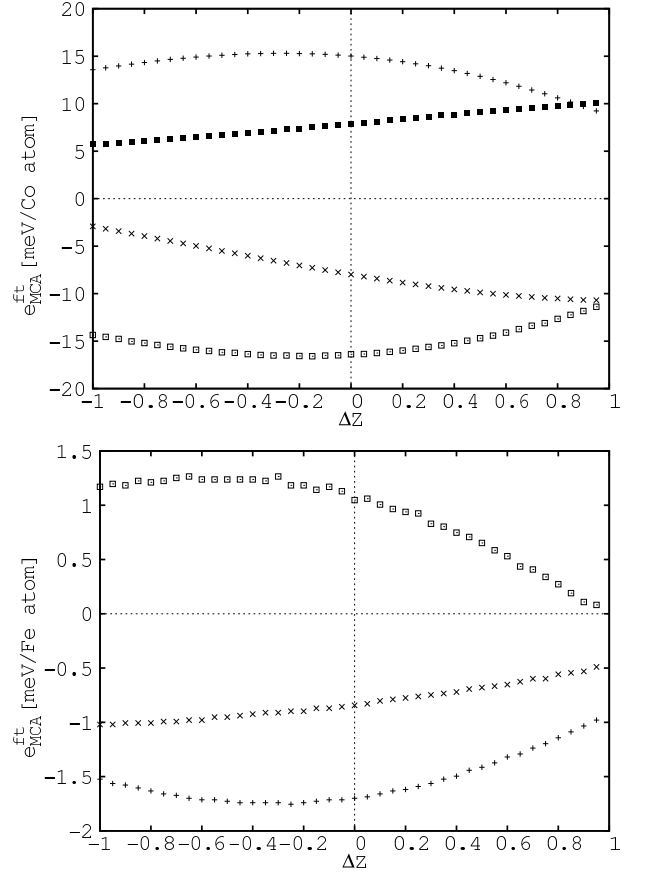


FIG. 6: The calculated magnetic anisotropy energy $e_{\text{MAE}}^{\text{ft}} = e(\theta = 0^\circ, \phi = 22.85^\circ) - e(\theta = 0^\circ, \phi = -67.15^\circ)$ for the Co wire (top) and $e_{\text{MAE}} = e(\theta = 0^\circ, \phi = 80.40^\circ) - e(\theta = 0^\circ, \phi = -9.60^\circ)$ for the Fe wire (bottom) projected to the Co (Fe) sites with SOC at all sites (+) or SOC just at the Co (Fe) sites (x), and projected to the Pt sites with SOC at all sites (□) or just at the Pt sites (■).

we want to distinguish between the “direct contribution” and the “indirect contribution” of the Pt atoms on the magnetic anisotropy by means of the methods (a) and (b) of Section 2.

From Figs. 4,5 it becomes obvious that there is a strong “direct contribution” $e_{\text{MCA}}^{\text{ft,Pt}}$ to the total anisotropy. Over a wide range of the Z values, the contributions of the Co(Fe) atoms and the Pt atoms are large but of opposite signs. For the Co wires the “direct contributions” from Co and Pt atoms nearly cancel each other, and the sum of the two contributions is close to the total anisotropy energy, indicating a small influence of the interstitial region. For the Fe wires the two direct contributions are much smaller than for the Co wire but the total anisotropy energy is of the same order of magnitude. The sum of $e_{\text{MCA}}^{\text{ft,Fe}}$ and $e_{\text{MCA}}^{\text{ft,Pt}}$ is drastically different from $e_{\text{MCA}}^{\text{ft}}$, indicating an unexpected large contribution of the interstitial region.

The plots in Figs. 2,3 clearly demonstrate that the

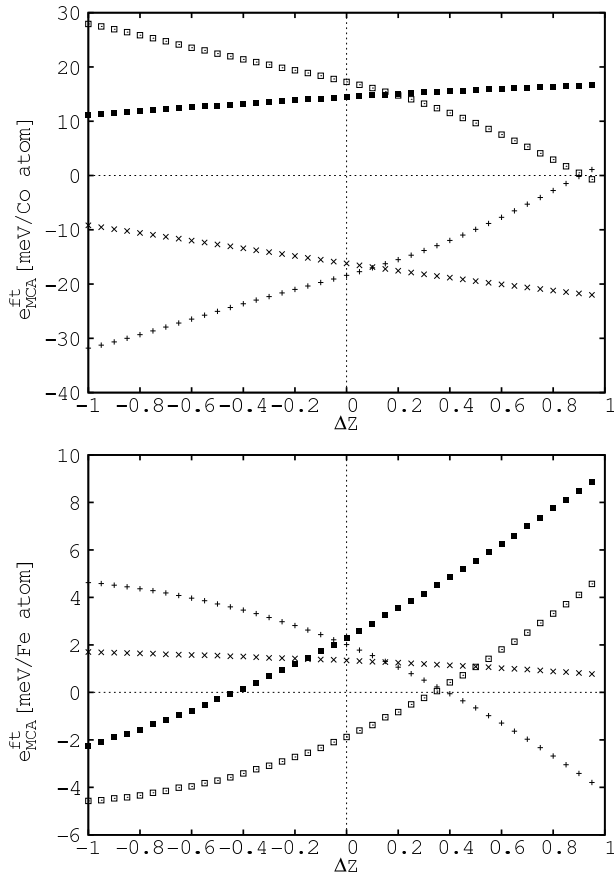


FIG. 7: The calculated magnetic anisotropy energy $e_{\text{MAE}} = e(\theta = 0^\circ, \phi = 0^\circ) - e(\theta = 90^\circ, \phi = 0^\circ)$ for the Co (top) and the Fe wire (bottom) projected to the Co (Fe) sites with SOC at all sites (+) or SOC just at the Co (Fe) sites (x), and projected to the Pt sites with SOC at all sites (□) or just at the Pt sites (■).

magnetic anisotropy of the Pt-supported Fe wires is strongly dominated by the SOC at the Pt atoms. In

the absence of this coupling, only a small magnetic anisotropy originating from the SOC at the Fe sites remains. In contrast, to obtain the magnetic anisotropy of the Pt-supported Co wires, we have to take into account the SOC for both the Pt and the Co atoms. Switching on the SOC term at the Pt atoms modifies both $e_{\text{MCA}}^{\text{ft,Co}}$ ($e_{\text{MCA}}^{\text{ft,Fe}}$) and $e_{\text{MCA}}^{\text{ft,Pt}}$. The modification of $e_{\text{MCA}}^{\text{ft,Co}}$ ($e_{\text{MCA}}^{\text{ft,Fe}}$) represents the “indirect contributions” of Pt atoms (see (b) of section 2). Figs. 6,7 represent the contribution $e_{\text{MCA}}^{\text{ft,Co}}$ (top) and $e_{\text{MCA}}^{\text{ft,Fe}}$ (bottom) together with the respective contributions $e_{\text{MCA}}^{\text{ft,Pt}}$ on the one hand calculated with SOC switched on for both Co (Fe) and Pt atoms (corresponding to the curves shown in Figs. 4,5), and on the other hand calculated with SOC on the respective other atoms switched off. Obviously there is a big “indirect contribution” of the Pt atoms, i.e., a big change of $e_{\text{MCA}}^{\text{ft,Co}}$ ($e_{\text{MCA}}^{\text{ft,Fe}}$) when the SOC on Pt is switched off. The “indirect contribution” thereby is of the same order of magnitude as the “direct contribution”.

The Pt substrate has an influence also on other magnetic properties of the wires. For instance, we have considered a freestanding Fe biwire and Fe biwires at the step of a Pt substrate, both for a ferromagnetic and for an antiferromagnetic alignment of the magnetic moments on the two adjacent monatomic wires (within each wire the alignment was ferromagnetic). The energy difference between these two configurations was about -20 mRy per Fe atom for the free-standing biwire and only about -7.7 mRy per Fe atom for the Pt supported biwire. For comparison, the difference in energy between the ferromagnetic and the antiferromagnetic configuration in bcc Fe at the equilibrium lattice constant of Pt is about -25 mRy/atom. The magnetic moment of the Fe atom for the Pt-supported biwire was very similar to the one of the Pt-supported monatomic wire.

We are indebted to G. Bihlmayer and A. B. Shick for helpful discussions and for providing their data and results.

* Electronic address: matej.komelj@ijs.si

¹ P. Gambardella, A. Dallmeyer, K. Maiti, M. C. Malagoli, W. Eberhardt, K. Kern, and C. Carbone, *Nature* **416**, 301 (2002).

² M. Komelj, C. Ederer, J. W. Davenport, and M. Fähnle, *Phys. Rev. B* **66**, 140407(R) (2002).

³ C. Ederer, M. Komelj, and M. Fähnle, *Phys. Rev. B* **68**, 052402 (2003).

⁴ J. Hong and R. Q. Wu, *Phys. Rev. B* **67**, 020406(R) (2003).

⁵ B. Lazarovits, L. Szunyogh, and P. Weinberger, *Phys. Rev. B* **67**, 024415 (2003).

⁶ B. Újfalussy, B. Lazarovits, L. Szunyogh, G. M. Stocks, and P. Weinberger, *Phys. Rev. B* **70**, 100404 (2004).

⁷ A. B. Shick, F. Máca, and P. M. Oppeneer, *Phys. Rev. B* **69**, 212410 (2004).

⁸ A. B. Shick, F. Máca, and P. M. Oppeneer, *J. Magn. Magn.*

Mater. **290-291**, 257 (2005).

⁹ F. Máca, A. B. Shick, J. Redinger, and P. M. Oppeneer, *Czech J. Phys.* **56** (2006).

¹⁰ G. Bihlmayer, in *Magnetism goes Nano: Proceedings of 36th IFF Spring School*, edited by S. Baud, Ch. Ramseier, G. Bihlmayer, and S. Blügel (Jülich, 2005).

¹¹ E. Wimmer, H. Krakauer, M. Weinert, and A. J. Freeman, *Phys. Rev. B* **24**, 864 (1981).

¹² P. Blaha, K. Schwarz, P. Sorantin, and S. B. Trickey, *Comput. Phys. Commun.* **59**, 399 (1990).

¹³ J. P. Perdew and Y. Wang, *Phys. Rev. B* **45**, 13244 (1992).

¹⁴ D. J. Singh, *Plane Waves, Pseudopotentials and the LAPW Method* (Kluwer Academic, Dordrecht, 1994).

¹⁵ P. Novák, unpublished.

¹⁶ A. R. Mackintosh and O. K. Andersen, in *Electrons at the Fermi Surface*, edited by M. Springford (Cambridge

- University Press, Cambridge, 1980).
- ¹⁷ M. Weinert, R. E. Watson, and J. W. Davenport, Phys. Rev. B **32**, 2115 (1985).
- ¹⁸ O. K. Andersen, Phys. Rev. B **12**, 3060 (1975).
- ¹⁹ P. E. Blöchl, O. Jepsen, and O. K. Andersen, Phys. Rev. B **49**, 16223 (1994).
- ²⁰ C.-L. Fu and K.-M. Ho, Phys. Rev. B **28**, 5480 (1983).